Science of Sintering, **49** (2017) 419-429

doi: https://doi.org/10.2298/SOS1704419J

UDK 692.533.1, 531.3

Ecologically Friendly Chitosan-montmorillonite Bio-nanocomposite as Adsorbent for Textile Dyes from Aqueous Solutions

Nataša Jović-Jovičić[1*)], Predrag Banković[1], Zorica Mojović[1], Bojana Nedić-Vasiljević[2], Sanja Marinović[1], Tihana Mudrinić[1], Aleksandra Milutinović-Nikolić[1]

[1]University of Belgrade- Institute of Chemistry, Technology and Metallurgy, Center for Catalysis and Chemical Engineering, Njegoševa 12, Belgrade, Serbia

[2]University of Belgrade, Faculty of Physical Chemistry, Studentski trg 12-16, Belgrade, Serbia

Abstract:

The bio-nanocomposite of montmorillonite and natural biopolymer chitosan (C-MM) was synthesized. Intercalation of chitosan in form of monolayer into the interlamellar space of montmorillonite was confirmed by XRD and IR analysis. The adsorption of textile dyes: Acid Yellow 99 (AY99), Acid Orange 10 (AO10) and Reactive Black 5 (RB5) onto C-MM was investigated. The adsorption was performed with the respect to adsorption time, pH and initial dye concentration. The kinetics of adsorption obeyed pseudo-second-order of kinetics and was the most efficient in acidic pH. Langmuir model best described the adsorption of AY99 and AO10 , while RB5 adsorption isotherm was best fitted with Freundlich model.

Keywords: *Adsorption isotherms; Characterization; Chitosan-montmorillonite bio-nanocomposite; Textile dyes; Kinetics.*

1. Introduction

Textile dyes are widely used in everyday life. The disposal of waters contaminated with these dyes into natural aquatic recipients can be regarded as very harmful. Exposure to azo dyes also entails exposure to the component aromatic amines due to: breakdown of azo dyes and presence of aromatic amines as impurities (their intermediates or breakdown products). It was found that there is a strong relationship between exposure to aromatic amines and risk to human cancer [1]. Since dyes have a high degree of chemical and photolytic stability [2] adsorption can be regarded as an appropriate method for dye removal prior their release into rivers, lakes etc. [3, 4]. Clays are well known as efficient and inexpensive adsorbent of a great variety of inorganic pollutants [5]. In order to be successful adsorbent of different organic pollutants, including textile dyes, the clays must previously be organomodified [6-8]. The most common way to organomodify clays is to use quaternary alkylammonium cations (QAAC). The clays modified with QAAC showed good adsorption capacity toward textile dyes only if the loading of QAAC excesses the cation exchange capacity (CEC) of the starting clay [8]. However, if the amount of QAAC highly excesses CEC the desorption process might occur.

*) **Corresponding author:** natashajvc@gmail.com

Since QAAC showed certain toxicity toward some biological systems [9] the highly loaded QAAC-clays potentially could become the source of secondary pollution.

In this study, natural biopolymer chitosan was used for the organo-modification process in order to get the ecologically friendly material. Chitosan is a cationic biopolymer (poly-h(1,4)-2- amino-2-deoxy-d-glucose) obtained by deacetylation of chitin.

Chitin is the second most abundant and widespread biopolymer after cellulose. There are several literature data referring to the synthesis of the chitosan-montmorillonite composites [10-12]. The main reaction path of the chitosan – montmorillonite interaction is through intercalation process of biopolymer chains into interlamellar space of montmorillonite [10-12]. The intercalation is achieved through electrostatic interaction between positively charged ammonium groups of chitosan polymer and negative sites on montmorillonite surface [10-12]. The obtained chitosan-montmorillonite composites are known as non-toxic materials with high mechanical strength and hydrophilic character especially proved as good adsorbents for different anionic species [13].

The goal of this work was to synthesize bio-nanocomposite based on montmorillonite and natural biopolymer chitosan and evaluate as a possible adsorbent for anionic aromatic azo dyes.

2. Experimental

2.1. Materials

Starting material was Na-montmorillonite (Na-MM), purchased from The Source Clays Repository - The Clay Minerals Society, from New Castle formation, Crook County, Wyoming, USA. Specification of this clay (denoted by suppliers as SWy-2) contains the following data: specific density of clay is 2.2 g cm^{-3} and chemical composition given in (mass%) SiO_2 – 62.9; Al_2O_3 – 19.6; Fe_2O_3 – 3.35; FeO – 0.320; MgO – 3.05; CaO - 1.68; Na_2O – 1.53; K_2O – 0.530; TiO_2 – 0.090; MnO – 0.006; F – 0.111; P_2O_5 – 0.049; S – 0.050 [14].

High molar mass chitosan (deacetylated chitin or poly(D-glucosamine)) (av. M_W =342,500 g mol^{-1}) was supplied by Sigma-Aldrich and used as a bioorganic phase for bio-nanocomposite synthesis.

Textile dyes used as adsorbates were Acid Yellow 99 (AY99) [$C_{16}H_{12}CrN_4O_9S{\cdot}Na$], Acid Orange 10 (AO10) [$C_{16}H_{10}N_2O_7S2{\cdot}2Na$] and Reactive Black 5 (RB 5) [$C_{26}H_{25}N_5O_{19}S_6{\cdot}4Na$], all purchased from Sigma-Aldrich and used as received.

2.2. Synthesis of chitosan/montmorillonite bio-nanocomposite

Chitosan/montmorillonite bio-nanocomposite (C-MM) was obtained according to the procedure described by Monvisade and Siriphannon, 2009 [10]. 2.5 g of Na-MM was dispersed in 100.0 ml of distilled water and stirred approx. 60 min in order to enable clay swelling. The chitosan solution was obtained by dissolving 4.0 g of chitosan in 200.0 ml of 2% (v/v) acetic acid and stirring for 24 h. The pH of chitosan solution was adjusted to 4.9 using 0.1 M NaOH. This pH value was chosen in order to provide protonated amino groups in chitosan structure and make intercalation process possible. At the same time, this pH enables preservation of montmorillonite structure [11]. The chitosan solution was dropwise added into Na-MM suspension and after complete adding the suspension was vigorously stirred for 24 h at room temperature.

The obtained C-MM was separated from the liquid phase by centrifugation at 17000 rpm for 10 min and washed with distilled water until neutral pH. The obtained sample was centrifuged, air-dried at 50°C and ground to powder.

2.3. Methods

The X-Ray diffraction patterns of the powders of montmorillonite (MM) and chitosan-montmorillonite (C-MM) was obtained using a Philips PW 1710 X-ray powder diffractometer, equipped with a Cu anode (λ=0.154178 nm).

The ATR-IR spectra of chitosan, MM and C-MM were recorded using the Thermo Nicolet 6700 FT-IR Spectrophotometer with the Smart Orbit Diamond ATR (attenuated total reflectance) accessory.

The point of zero charge - pH_{PZC} for C-MM was obtained using the experimental method described by Čerović et al. [15]. The 25.0 mg of C-MM sample was shaken in 50 ml of a 0.01 M NaCl solution for 24 h. The initial pH values ($pH_{initial}$) were adjusted in the pH range from 2 to 12 by adding appropriate amounts of 0.1 M HCl or 0.1 M NaOH solution. After 24 h the suspension was centrifuged, and the final pH values of supernatants were measured (pH_{final}). The point of zero charges was determined from the $pH_{initial}$ vs. pH_{final} diagram.

Thermo Electron Nicolet Evolution 500 UV-VIS spectrophotometer was used for measurement of dye concentration. The concentration of each dye was estimated using calibration curves (R^2> 0.999) obtained for absorption maxima at λ_{max}=449 nm, 478 nm and 599 nm for AY99, AO10 and RB5, respectively. All adsorption experiments were carried out in triplicate, and average values are given in this manuscript. The relative standard deviation was lower than 0.1 %.

2.4. Adsorption experiments

Batch-type adsorption experiments were conducted in aqueous solutions in a temperature-controlled water bath shaker (Memmert WNE 14 and SV 1422). Adsorption was carried out with respect to contact time and initial dyes concentration. The aliquots were withdrawn from the shaker at regular time intervals and the solution was centrifuged at 17000 rpm for 10 min (Hettich EBA-21).

The experiments were carried out at 25°C, using the same mass of adsorbent (10.0 mg) and volume of solution (50.0 cm^3). The initial dye concentration was 50 mg dm^{-3} at pH=6. The influence of pH on dye removal was studied by adjusting initial solutions to different pH values (2–12) using a pH meter (PHM240 MeterLab®).The amount of dye adsorbed after time t - q_t (mg g^{-1}), was calculated from mass balance equation [7, 8].

3. Results and Discussion

3.1. Sample characterization

The XRD patterns of MM and C-MM are given in Figure 1. The XRD of the clay sample (Fig. 1a) shows the presence of quartz and feldspar along with Na-montmorillonite as the major component [16].

The d_{001} value increases from 1.20 nm (characteristic for Na-montmorillonite) to 1.52 nm for C-MM intercalated chitosan-montmorillonite structure of bio-nanocomposite [12]. According to the literature data, the values of 1.52 nm indicate monolayer arrangement of chitosan chains within interlamellar space of montmorillonite [12].

The intensity of the peak at 2θ=28.4° corresponding to feldspar present in diffractogram of MM decreased in diffractogram of C-MM (Fig. 1b). This finding is in accordance to previously reported literature data [17] reporting disappearance of this peak in the presence of chitosan in an acidic environment. The XRD data confirmed intercalation of

chitosan chains into interlamellar space of montmorillonite and successful synthesis of bio-nanocomposite.

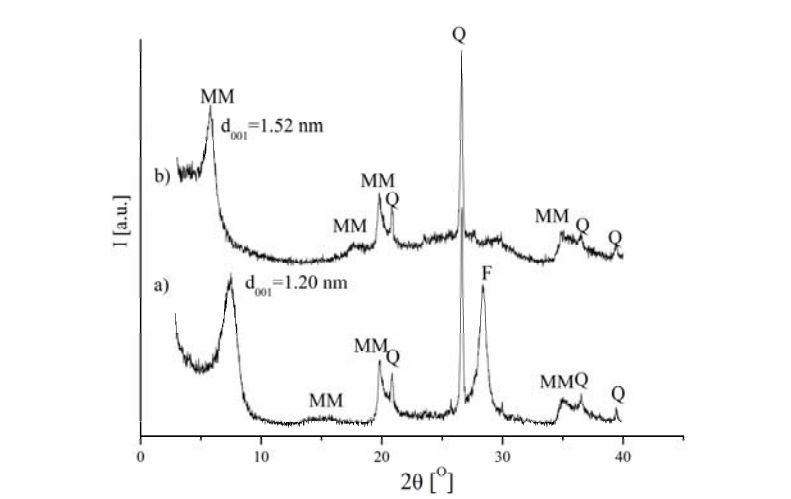

Fig. 1. XRD patterns of (a) MM and (b) C-MM; (S-smectite, F - feldpar, Q - quartz).

In Fig. 2 ATR-IR spectra of MM, C-MM, as well as chitosan film, are given.

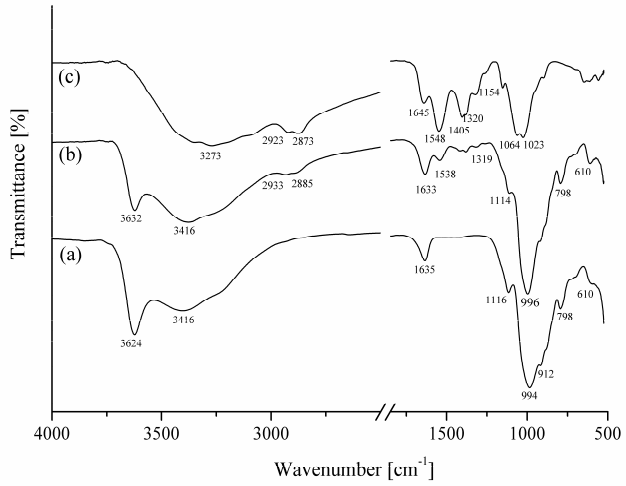

Fig. 2. IR spectra: (a) MM; (b) C-MM (c) Chitosan film.

In the spectrum of MM (Fig. 2 curve a) all bands were assigned to vibrations in montmorillonite, quartz and water. The broad band at about 3624 cm^{-1} was assigned to the stretching vibrations of the structural hydroxyl group of Na-montmorillonite. Broad bands around 3416 and 1635 cm^{-1} were attributed to the stretching and bending O–H vibrations in water molecules, respectively. The bands at 1116 cm^{-1} and 994 cm^{-1} are ascribed Si-O stretching longitudinal and valence vibration, respectively. The band at 912 was assigned to the bending vibrations of AlAlOH. The band at 798 cm^{-1} was attributed to Si-O stretching of quartz and silica, while the band at 610 cm^{-1} was assigned to coupled Al-O and Si-O out-of-plane bending vibration [18, 19].

The spectrum of chitosan film (Fig. 2, curve c) showed characteristic bands originated from O-H stretching and bending vibrations of pyranose ring at 3273 and 1645 cm^{-1}, respectively. The bands at 2923 and 2873 cm^{-1} were assigned to valence C-H vibrations, while bands at 1405 and 1320 cm^{-1} originated from C-H bending vibrations. Characteristic

bending vibrations of N-H was observed at 1548 cm^{-1}. The bands at 1154, 1064 and 1023 cm^{-1} were assumed to correspond to C-O-C stretching vibrations [12, 20, 21].

The spectrum of the C-MM (Fig. 2, curve b) shows both bands characteristic for chitosan and montmorillonite. The N-H bending vibration of chitosan film shifted from 1548 to 1538 cm^{-1} in C-MM, which is in accordance with literature data [12]. Such shift can be assigned to the interaction of ammonium groups in chitosan chains with negatively charged sites located in montmorillonite. The bands in the 1250-500 cm^{-1} region from different origin i.e. chitosan and montmorillonite overlap and are not discussed.

The results obtained pH_{PZC} value for C-MM was shown in Fig. 3. The pH_{PZC} value of 6.5 for the C-MM bio-nanocomposite was determined as the pH_{final} level where a common plateau was obtained. This result indicated that when the pH of the solution is below pH =6.5 the adsorbent surface has a positive charge, while above this value the surface charge is negative.

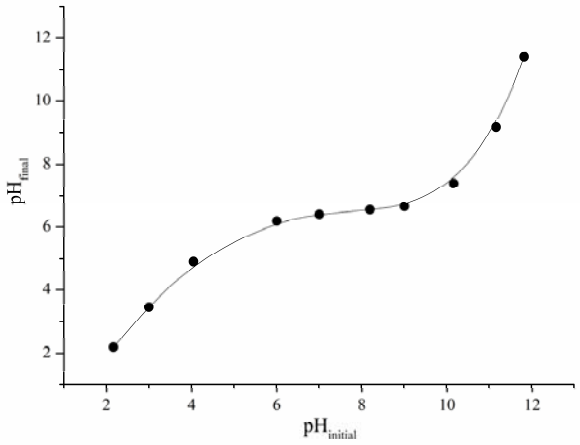

Fig. 3. Determination of the point of zero charge (pH_{PZC}) of C-MM bio-nanocomposite.

3.2. Adsorption results

3.2.1. The effect of contact time

The effect of contact time on the adsorption of different dyes onto C-MM was shown in Fig. 4.

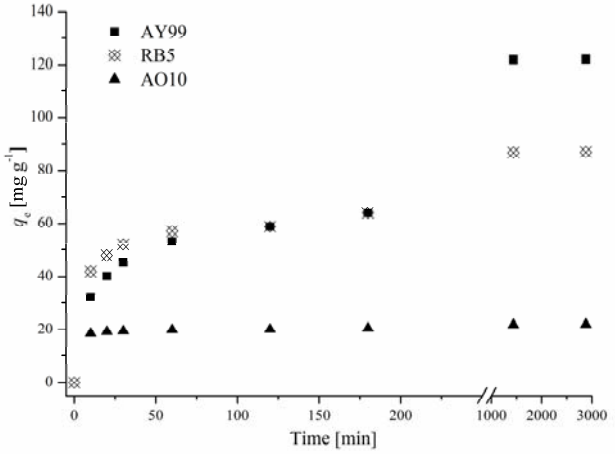

Fig. 4. The effect of contact time on the adsorption of AY99, RB5 and AO10 on C-MM.

The Fig. 4. showed that C-MM had different adsorption affinity toward the investigated dyes in the following order: AY99 > RB5 > AO10. In the first 60 min AY99, RB5 and AO10 43%, 78% and 97% were adsorbed, respectively. In the case of AO10, 60 min can be regarded as equilibrium time since afterward no further adsorption was observed. On the other hand, for AY99 and RB5 only after 1440 min the amount of adsorbed dye remained almost constant. The further extent of contact time did not change the amount of adsorbed dye and no desorption process under-investigated conditions were observed. The amount of adsorbed dye for AO10, RB5 and AY99 at equilibrium time was 21.9, 87.1 and 121.8 mg g^{-1}, respectively.

The adsorption rates of AO10, RB5 and AY99 were tested using pseudo-first-order and pseudo-second-order kinetics models [22]. The parameters calculated for both models and all dyes onto C-MM are presented in Table I.

Tab. I Pseudo-first-order kinetic and pseudo-second-order kinetics for the adsorption of AY99, RB5 and AO10 onto C-MM.

	AY99	**RB5**	**AO10**
q_e^{exp} **(mg g^{-1})**	121.8	87.1	21.9
Pseudo-first-order kinetic model			
q_e^{calc} **(mg g^{-1})**	96.5	35.2	2.69
k_1 **(min^{-1})**	$4.4 \cdot 10^{-3}$	$2.5 \cdot 10^{-3}$	$2.1 \cdot 10^{-3}$
R^2	0.996	0.985	0.979
Pseudo-second-order kinetic model			
q_e^{calc} **(mg g^{-1})**	128.2	84.0	20.6
$k_2 \times 10^2$ **(g $mg^{-1}min^{-1}$)**	$9.2 \cdot 10^{-3}$	$1.3 \cdot 10^{-3}$	$2.9 \cdot 10^{-2}$
R^2	0.999	1	1

k_1 – pseudo-first-order rate constant (min^{-1}); k_2 – pseudo-second-order rate constant; q_e^{exp} – experimentally obtained value for the equilibrium adsorption capacity; q_e^{calc} – calculated value for the equilibrium adsorption capacity; R^2 – square of coefficients of correlation.

Squares of coefficients of correlation (R^2) for all investigated adsorbates were lower for the pseudo-first-order kinetics model than corresponding coefficients for pseudo-second-order kinetics model ($R^2 \geq 0.999$). The calculated value for the equilibrium adsorption capacity q_e^{calc} for pseudo-second-order kinetics model for all samples exhibited a high degree of agreement with experimentally obtained adsorption capacity, q_e^{exp}, confirming that the adsorption of investigated dyes onto C-MM obeyed the pseudo-second-order kinetics.

According to Plazinski et al. [23], the pseudo-second-order model describes adsorption process where the limiting rate step can be controlled by two factors: (i) transfer of adsorbate through adsorbent – solution boundary layer or (ii) intraparticle diffusion process. It was also shown that for pseudo-second-order kinetic reactions, the intraparticle diffusion model can be applied for both spherical and plane-like adsorbent particles, as well as systems with homogeneous and heterogeneous solid surfaces.

The intraparticle diffusion model was applied to the experimentally obtained kinetic data for AY99, RB5 and AO10 adsorption onto C-MM. The equation that describes intraparticle diffusion model in linear form is given by Weber and Morris [24].

The plots q_t vs. $t^{0.5}$ for adsorption of AY99 and RB5 onto C-MM were shown in Fig 5.

The adsorption process for AO10 was fast with $t_{1/2}$ = 6.5 min ($t_{1/2}$ – time at which the half of amount of adsorbed AO10 at the equilibrium) estimated from the graph in Fig. 4. Therefore the intraparticle diffusion model is not applicable for this dye.

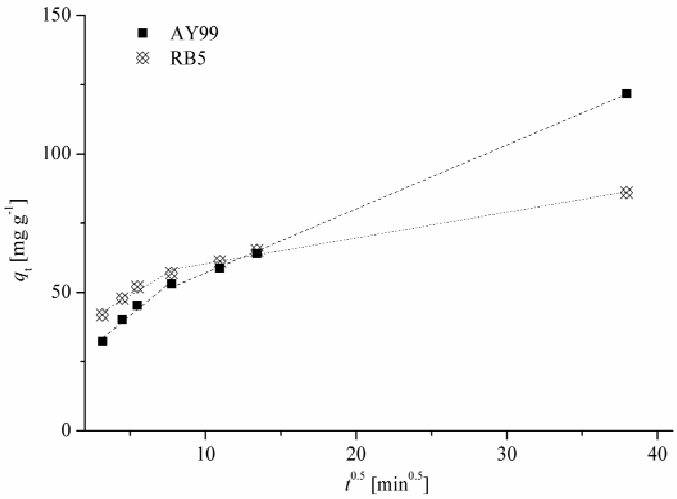

Fig. 5. Intraparticle diffusion model for AY99 and RB5.

The intraparticle diffusion model parameters were calculated based on linear plots and given at Table II.

Tab. II The intraparticle diffusion parameters for adsorption of AY99 and RB5 onto C-MM.

ID parameters	**AY99**	**RB55**
C_{id} **(mg g^{-1})**	19.3	32.7
$k_{id,1}$ **(mg g^{-1} min$^{-0.5}$)**	4.47	3.25
R_1^2	0.965	0.945
$k_{id,2}$ **(mg g^{-1} min$^{-0.5}$)**	2.3	0.93
R_2^2	0.999	0.991

C_{id} – boundary layer adsorption rate; $k_{id,1}$, $k_{id,2}$ – diffusion rates constant.

From Fig. 5. and Table II it could be noticed that there were two linear parts of the adsorption of AY99 and RB5 onto C-MM. According to the literature [25], if the linear plot of q_t vs. $t^{0.5}$ does not pass through the origin, the intraparticle diffusion is not the only rate-controlling stage and external mass transfer is involved in the adsorption process. The intercept values (C_{id}) for both AY99 and RB5 (Table II) are positive indicating that boundary layer influenced the adsorption rate. The intraparticle diffusion constants, $k_{id,1}$ and $k_{id,2}$ were calculated from the slope of the corresponding linear regions (Fig. 5.). The $k_{id,1}$ and $k_{id,2}$ express diffusion rates of the two different adsorption stages. The assumption is that the dye molecules were firstly adsorbed onto the exterior surface of C-MM particles. At this stage the adsorption is faster, which could be confirmed by comparing higher $k_{id,1}$ value to $k_{id,2}$. When the adsorption onto the outer surface was completed, the dye molecules diffuse into particles and adsorb onto inner surface.

3.2.2. The effect of pH

The influence of the initial pH value of AY99, RB5 and AO10 solutions on the adsorption onto C-MM is shown in Fig. 6. The adsorptions take place 60 min with a dye concentration of 50 mg dm^{-3} in pH range 2 – 12.

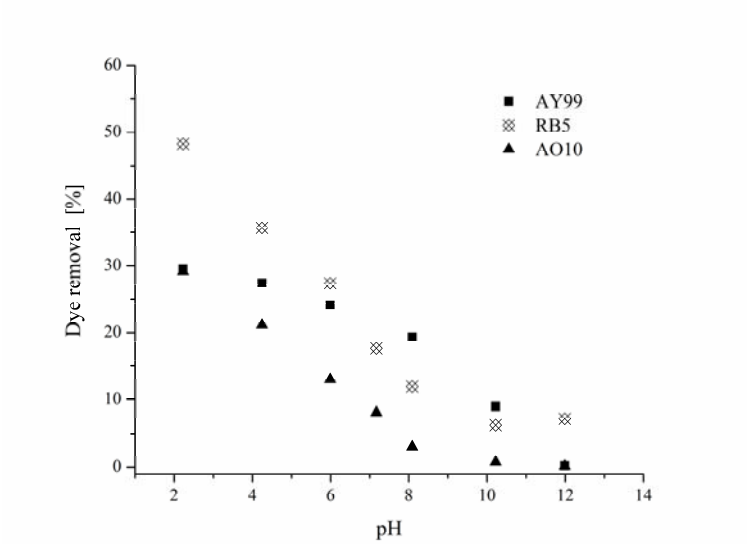

Fig. 6. The effect of the initial pH of AY99, RB5 and AO10 solutions on the adsorption onto C-MM.

The pH has a high impact on the adsorption of the investigated dyes. Adsorption of all three dyes showed a similar trend: the highest percent of dye removal was obtained in acidic medium. When the pH value of dye solution raised from 2 to 8 the percent of dye removal linearly decreased from 29.6 to 19.3, 48.3 to 11.2 and 29.1 to 3.0% for AY99, RB5 and AO10, respectively. Further increase of the pH value of dye solutions leads to an additional decrease of dye removal. In highly alkaline medium the adsorption still exists only for RB5. The higher removal of dyes at lower pH values can be attributed to electrostatic attraction between protonated active sites of C-MM (positive charged C-MM at pH below pH_{PZC}=6.5) with anionic groups of dyes. When the initial pH of the solution increased, the positive charge of C-MM surface decreased and the negatively charged surface became dominant, leading to electrostatic repulsion. The obtained results are in accordance with trends observed in the literature for similar adsorption systems [26, 27].

3.2.3. Adsorption isotherms

The Langmuir model [28] is widely applied adsorption isotherm. It is based on the following assumptions: (i) adsorbing sites are equivalent and distributed homogenously on the surface and (ii) only monolayer coverage could be formed. The Freundlich model [29] is empirical and can be applied to multilayer adsorption on energetically heterogeneous surfaces. Both models describe chemisorption and physisorption processes.

The adsorption isotherms for AY99, AO10 and RB5 adsorption onto C-MM were obtained using different initial dye concentration in the range 10.0 – 60.0 mg dm^{-3}. The parameters calculated according to Langmuir and Freundlich isotherm model are presented in Table III.

For the adsorption of AY99 and AO10 onto C-MM, squares of correlation coefficients (R^2) have shown better agreement with Langmuir isotherm model than Freundlich. Although for the adsorption of RB5 the R^2 for Freundlich's isotherm model was higher than Langmuir's, the latter was still appropriate (R^2=0.952) for further discussion. The

Langmuir model predicted theoretical values of the adsorption capacity of 196.6, 97.1 and 44.5 mg g^{-1} for AY99, RB5 and AO10, respectively. The explanation for different adsorption capacity of C-MM toward investigated dyes could be proposed according to dye structures [30].

The electrostatic interaction between adsorbent surface and anionic $-SO_3^-$ groups of dyes could be the major contribution to the adsorption of all dyes [26]. C-MM showed the highest adsorption capacity for AY99. This finding could be related to the presence of coordinative bonded Cr^{3+} in AY99 structure. It is well known that chitosan is a good chelating agent for cations of transition metals [31] and therefore the presence of Cr^{3+} could significantly contribute to the interaction with the C-MM. On the other hand, the better adsorption capacity for RB5 in comparison to AO10 probably can be ascribed to the presence of four and two $-SO_3^-$ groups in RB5 and AO10 molecules, respectively.

Tab. III Parameters calculated for the Langmuir and Freundlich isotherm models.

	AY99	RB5	AO10
Langmuir isotherm			
q_{max} (mg g^{-1})	196.6	97.1	44.5
K_L (dm^3 mg^{-1})	0.07	34.2	0.02
R^2	0.997	0.952	0.962
Freundlich isotherm			
n	1.98	10.99	1.58
K_F (dm^3 mg^{-1})	24.4	60.2	1.89
R^2	0.989	0.994	0.946

q_{max} – maximum adsorption capacity; K_L – Langmuir adsorption constant; K_F – Freundlich adsorption constants; n – Freundlich adsorption constants

QAAC-clays showed either lower or higher adsorption capacities toward investigated dyes than C-MM depending on QAAC loading. [8, 30]. However, it was found that C-MM is better than some of previously reported adsorbents: (i) q_{max} of AO10 was higher than reported for CeO_2 nanoparticles and Bagasse fly ash, 33.3 mg g^{-1} [32] and 18.8 mg g^{-1} [33], respectively; (ii) q_{max} of AY99 was higher than for diethylenetriamine functionalized magnetic glycidyl methacrylate q_{max}=124.1 mg g^{-1} [34] and (iii) q_{max} of RB5 was higher than activated carbon and fly ash with q_{max} of 58.8 mg g^{-1} and 7.9 mg g^{-1}, respectively [35].
These findings qualify chitosan-montmorillonite bio-nanocomposite as potentially applicable ecologically friendly adsorbent for the investigated textile dyes.

4. Conclusion

The bio-nanocomposite of montmorillonite and natural biopolymer chitosan (C-MM) was synthesized. Intercalation of chitosan polymer chains into interlamellar space of montmorillonite was confirmed by XRD. The d_{001} value of 1.52 nm detected for C-MM indicated incorporation of chitosan in monolayer form. The IR spectrum of the C-MM showed bands characteristic for chitosan and montmorillonite. The presence of the band attributed to N-H bending at 1538 cm^{-1}confirmed interaction of ammonium groups in chitosan chains with negatively charged sites located in montmorillonite. The pH_{PZC} value for the C-

MM bio-nanocomposite was 6.5.

The adsorption properties of C-MM were investigated using three textile dyes: Acid Yellow 99 (AY99), Acid Orange 10 (AO10) and Reactive Black 5 (RB5). Adsorption of all investigated dyes obeyed pseudo-second-order kinetics. The intraparticle model for AY99 and RB5 indicated that intraparticle diffusion boundary layer mainly influenced the adsorption rate. The effect of pH of the initial dyes solutions showed that the adsorption of the investigated dyes was the most efficient in acidic pH. The adsorption isotherms for AY99 and AO10 are well described by Langmuir model, while RB5 adsorption isotherm was best fitted with Freundlich model. C-MM had different adsorption affinity toward investigated dyes in the following order: AY99 > RB5 > AO10. The observed differences could be correlated with the dye structures.

Based on results obtained in this study, the C-MM bio-nanocomposite could be potentially applicable adsorbent for the investigated textile dyes.

Acknowledgment

This work was supported by the Ministry of Education, Science and technological Development of the Republic of Serbia (Project III 45001).

5. References

1. K. T. Chung, Carcino. Ecotox. Revs., 18 (2000) 51.
2. C. R. Nony, M. C. Bowman, J. Anal. Toxicol., 4 (1980) 63.
3. S. Nenadović, Lj. Kljajević, S. Marković, M. Omerašević, U. Jovanović, V. Andrić, I. Vukanac, Sci. Sinter., 47 (2015) 299.
4. D. O. Cooney, Adsorption Design for Wastewater Treatment, Lewis Publishers, Boca Raton, 1999.
5. H. B. Bradl, J. Colloid Interf. Sci., 277 (2004) 1.
6. S. Marinović, M. Ajduković, N. Jović-Jovičić, P. Banković, Z. Mojović, A. Milutinović-Nikolić, D. Jovanović, Sci.Sinter., 48 (2016) 167.
7. N. Jović-Jovičić, A. Milutinović-Nikolić, P. Banković, Z. Mojović, M. Žunić, I. Gržetić, D. Jovanović, Appl. Clay Sci., 47 (2010) 452.
8. N. Jović-Jovičić, A. Milutinović-Nikolić, M. Žunić, Z. Mojović, P.Banković, I. Gržetić, D. Jovanović, J. Contam. Hydrol., 150 (2013) 1.
9. U. Tezel, Fate and effect of quaternary ammonium compounds in biological systems, Ph.D. Thesis, Georgia Institute of Technology, 2009. https://smartech.gatech.edu/bitstream/handle/1853/28229/tezel_ulas_200905_phd.pdf (verified March 2017)
10. P. Monvisade, P. Siriphannon, Appl.Clay Sci., 42 (2009) 427.
11. M. Darder, M. Colilla, E. Ruiz-Hitzky, Appl. Clay Sci., 28 (2005) 199.
12. M. Darder, M. Colilla, E. Ruiz-Hitzky, Chem. Mater., 15 (2003) 3774.
13. E. Ruiz-Hitzky, P. Aranda, M. Darder, G. Rytwob, J. Mater. Chem., 20 (2010) 9306.
14. Clay Minerals Society, Source Clay Physical/Chemical Data. http://www.clays.org/Sourceclays.html (verified March 2017).
15. Lj. Čerović, S. K. Milonjić, M. Todorović, M. Trtanj, Y. Pogozhev, Y. Blagoveschenskii, E. A. Levashov, Colloid Surf. A, 297 (2007) 1.
16. International Center for Diffraction Data, Joint Committee on Powder Diffraction Standards JCPDS, 1990, Swarthmore, USA.
17. M. Yazdani, H. Bahrami, M. Arami, Sci. World J., ID 370260 (2014) 13.

18. Madejová, J., Komadel, P., Čičel, B., Clay Miner., 29 (1994) 319.
19. Madejová, J., Komadel, P., Clays Clay Miner., 49 (2001) 410.
20. N. Jović-Jovičić, Z. Mojović, M. Darder, P. Aranda, E. Ruiz-Hitzky, P. Banković, D. Jovanović, A. Milutinović-Nikolić, Appl. Clay Sci., 124 (2016) 62.
21. J. Kumirska, M. Czerwicka, Z. Kaczyński , A. Bychowska, K. Brzozowski, J. Thöming, P. Stepnowski, Mar. Drugs, 8 (2010) 1567.
22. S. Lagergren, „Zur theorie der sogenannten adsorption gelöster stoffe", Kungliga Svenska Vetenskapsakademiens, Handlingar 24 (1898) 1.
23. W. Plazinski, J. Dziuba, W. Rudzinski, Adsorption, 19 (2013) 1055.
24. W. J. Weber Jr., J. C. Morris, J. Sanit. Eng. Div. Am. Soc. Civ. Eng., 89 (1963) 31.
25. A. Özcan, A. S. Özcan, J. Hazard. Mater., B125 (2005) 252.
26. L.Wang, A. Wang, J. Hazard. Mater., 147 (2007) 979.
27. C. Umpuch, S. Sakaew, Songklanakarin J. Sci. Technol. 35 (2013) 451.
28. I. J. Langmuir, J. Am. Chem. Soc., 40 (1918) 1361.
29. H. M. F. Freundlich, J. Phys. Chem., 57 (1906) 385.
30. N. Jović-Jovičić, A. Milutinović-Nikolić, M. Žunić, Z. Mojović, P. Banković, B. Dojčinović, A. Ivanović-Šašić, D. Jovanović, J. Serb. Chem. Soc. 79 (2014) 1.
31. W. S. Wan Ngah, L. C. Teong, M. A. K. M. Hanafiah, Carbohydr. Polym. 83 (2011) 1446.
32. H. Budiman, O. Zuas, Indo. J. Chem., 14 (2014) 226.
33. I. D. Mall, V. C. Srivastava, N. K. Agarwal, Dyes Pigm., 6 (2006) 210.
34. K. Z. Elwakeel, A. A. El-Bindary, A. Z. El-Sonbatib, A. R. Hawas, RSC Adv., 6 (2016) 3350.
35. Z. Eren, F.N. Acar, Desalination, 194 (2006) 1.

Садржај: *Бионанокомпозит монморијонита и природног биополимера хитозана (C-MM) је синтетисан. Интеркалација хитозана у интерламеларни простор монморијонита у облику монослоја је потврђена рендгено-структурном анализом и инфрацрвеном спектроскопијом.*

Испитивана је адсорпција текстилних боја Acid Yellow 99 (AY99), Acid Orange 10 (AO10) и Reactive Black 5 (RB5) на C-MM. Испитиван је утицај времена, pH вредности почетног раствора боје и почетне концентрације боја на адсорпцију. Утврђено је да кинетика адсорпције одговара моделу псеудо-другог реда. Адсорпционе изотерме за боје AY99 и AO10 најбоље могу бити описане Лангмировим адсорпционим моделом, док се адсорпција боје RB5 најбоље слаже са Фројндлиховим моделом.

Кључне речи*: адсорпционе изотерме, карактеризација, хитозан-монморијонит бионанокомпозит, текстилне боје, кинетика.*